



PM₁₀ and the Air Quality Stress Index in an industrial city of Eastern Mediterranean

Eleni Verouti¹, Dimitrios Gavathas² and Anastasios Mavrakis³ 

¹ Bureau of Environment and Civil Protection, Municipality of Aspropyrgos, Aspropyrgos – Attica, Greece

² Department of Chemistry, University of Patras, Rio Patras, Greece

³ West Attica Secondary Education Directorate, Greek Ministry of Education, Elefsis – Attica, Greece

Received 27 July 2021, in final form 7 December 2021

The contribution of PM₁₀ to the daily Air Quality Stress Index (AQSI) was examined in a heavily affected industrial city of Eastern Mediterranean (Aspropyrgos, Greece). For this purpose, hourly concentration values of four pollutants (SO₂, NO₂, O₃, and PM₁₀) were analyzed between 2012 and 2020, revealing that the main contributor to AQSI levels came from PM₁₀ (between 17% and 90% to the daily AQSI), with a moderate annual variability and a spring peak. Excluding PM₁₀, the AQSI always remained below the threshold of 0.8. To identify the atmospheric source of PM₁₀ peaks, the Flextra – Air mass trajectories model was applied to 47 cases in which the upper threshold was exceeded. The results of the model show that dust transport episodes, mainly from Sahara Desert, contribute to the daily levels of PM₁₀ and, accordingly, to AQSI.

Keywords: PM₁₀, Air Quality Stress Index, dust transport episodes

1. Introduction

The first and main industrial area of Greece is located in West Attica Prefecture, west-northwest of Athens, the capital city of Greece, which hosts 40% of the country's population. The prefecture has the industrialized Thriasio Plain as the core area located 20 km northwest of Athens, including three municipalities, namely Aspropyrgos, Elefsis and Mandra, along with the community of Magoula (Figs. 1a and 1b). The topography is mostly flat, with a gentle slope towards the sea not exceeding 3%. This basin encompasses an area of 500 km² and houses a total population of 120,000 inhabitants (2011 census, ELSTAT, 2011). The presence of several mountains, close to the sea, the local climatic conditions (Mavrakis et al., 2015b), and the unfavourable topography, produce

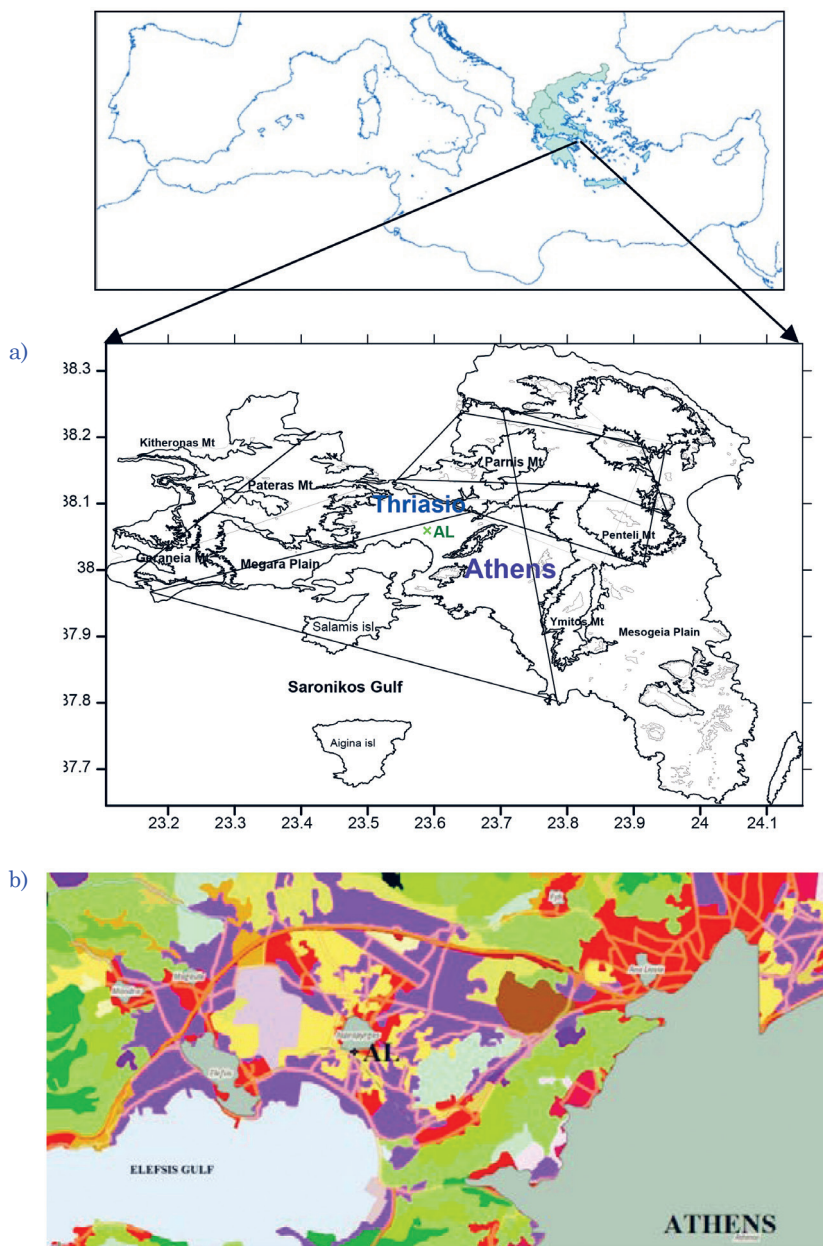


Figure 1. *a)* Map of Attica prefecture, where Thriasio Plain and Athens basins and the air quality station of Alonistra (AL) – Municipality of Aspropyrgos, are shown. *b)* Urban Atlas – European Environment Agency (EEA, 2016) land-use map: industrial/commercial areas are displayed in purple, urban areas in red, rural areas in yellow, bare land in beige, vegetated land is displayed with different shades of green and light gray for the legislated municipalities plan.

local regressive atmospheric circulation patterns (Lykoudis et al., 2008) that inhibit the capability of atmospheric self-cleaning through dispersion and transport mechanisms (Mavrakis et al., 2008). Temperature inversion heights are especially low during the cold seasons of the year, frequently being lower than the surrounding hills and comparable to the heights of the highest chimneys characteristics of the large industrial compounds in the area. Even more, the sea shore is occupied by various industries, as well as other (authorized and informal) activities, which actually act as a wall between the shallow Elefsis Gulf and the inside plain (Mavrakis et al., 2008). This means that air pollutants are trapped within a shallow layer, resulting to high (daily and hourly) air pollutants' concentrations. The Thriasio Plain exhibits the higher: (a) industrial activity concentration, (b) fuel consumption and (c) pollution, related to the production processes in Greece (Abatzoglou et al., 1996; Lykoudis et al., 2008; Mavrakis et al., 2008). Mavrakis et al. (2016) quantified the industrial asset of the area in (at least) 6,500 large and small industrial plants, including all kinds of industries, such as oil refineries, chemical and steel production, metal and non-metal minerals' processing, cement industries and logistics (Fig. 1b). Apart from the industrial activities, the area is crossed by three freeways (two national roads and, since 2003, a large part of the urban freeway "Attiki Odos"), as well as by two railroad lines (the national railway line and, since 2005, the Athens' suburban railway). Furthermore, nine large quarries are actually under operation, and the 13 docks of Elefsis harbour accommodate 5,500 ships per year, with a total cargo load 2.5 times larger than that handled by the Piraeus harbour (the major one of Greece).

The municipality of Aspropyrgos houses about 35,000 inhabitants and receives the largest number of all kinds of established activities (2,700 out of a total of 6,500; Fig. 1b), around the municipal centre (Di Felicianantonio et al., 2018), thanks to the large availability of flat and fertile free land (both public and private) around the urban core of the city, contrary to the surrounding municipalities (Mavrakis et al., 2016).

For the air quality of the nearby Athens, the Thriasio Plain has been frequently regarded as a pollution source. However, a relatively limited number of studies considering air pollution issues, although pollution levels have been identified as serious, since the early 1990 (Abatzoglou et al., 1996; Kassomenos et al., 2004; Lykoudis et al., 2008; Mavrakis et al., 2008; Toumpos et al., 2017). Koukoulakis et al., (2019) and Kanellopoulos et al. (2021) have given special attention to primary and secondary organic aerosol and to trace elements bound to PM_{10} in the area as well as to their possible health implications.

The present study examines trends in air quality over the city of Aspropyrgos, which is located at the centre of Thriasio Plain, using a composite index derived from the levels of four pollutants recorded in the area (namely SO_2 , NO_2 , O_3 , and PM_{10}), by using the complete hourly and daily data set, collected by the local air-quality monitoring station during the time period 2012–2020. The con-

tribution of PM₁₀ to the daily Air Quality Stress Index (AQSI) was finally examined. The Flextra – Air mass trajectories model was used to identify the atmospheric source of elevated PM₁₀ peaks in all cases when the AQSI upper thresholds were exceeded.

2. Methods

The data used in this study were provided by Alonistra (AL) air pollution monitoring station, located in Aspropyrgos town (500 m south of the city centre and 1500 m from the sea shore) and operated by the Bureau of Environment, Municipality of Aspropyrgos (BEMA). Hourly values of air temperature (T_a , °C), relative humidity (RH, %) and concentrations ($\mu\text{g}/\text{m}^3$) of sulphur dioxide (SO₂), nitrogen dioxide (NO₂), ozone (O₃) and particulate matter less than 10 μm in diameter (PM₁₀), as recorded for the 2012–2020 time periods, were collected and analyzed here.

In European Union (EU), although member states are subject to the same directives in respect of air quality, the use of a common Air Quality Index (AQI) has not been adopted, with most countries applies their own AQI. This is because AQIs were developed in most of countries and thus have been adapted to technical requirements, quality standards and Knowledge needs of the investigated area (Karavas et al., 2021).

For the purpose of this study, air quality was assessed using the daily Air Quality Stress Index (AQSI). This methodology was firstly applied in SW Germany by Mayer et al. (2004) and also in Athens by Katsoulis and Kassomenos (2004) and Kassomenos et al. (2012). Air Quality Stress Index give an overall assessment of air quality, including the synergetic effects of the recorded air pollutants, is based on an arithmetic summation of relative concentrations of air pollutants and can be considered a summary assessment of the ambient air pollution. According to Mayer et al. (2004), Katsoulis and Kassomenos (2004) and Kassomenos et al. (2012) the typical structure is given by the formula:

$$AQSI = \frac{1}{n} \sum_{i=1}^n \frac{Ci - \text{average} - \text{daily} - \text{values}}{MI - 24h - \text{values}_i}, \quad (1)$$

where n is the number of air pollutants, C_i is the time-specific concentration, and $MI - 24h$ value indicates the threshold of air pollutant concentration, Based on the threshold values, the equation (1) can be rewritten as follows:

$$AQSI = \frac{1}{4} \left[\frac{C(\text{SO}_2)}{350} + \frac{C(\text{NO}_2)}{200} + \frac{C(\text{O}_3)}{180} + \frac{C(\text{PM}_{10})}{50} \right], \quad (2)$$

where C indicates the concentration of the respective pollutant expressed in $\mu\text{g}/\text{m}^3$. $C(\text{SO}_2)$ and $C(\text{NO}_2)$, are the daily maximum 1-h concentrations; $C(\text{O}_3)$ is the daily maximum 8-h running mean concentration and $C(\text{PM}_{10})$ is the daily

mean concentration value. The denominators stand for the upper limit values set by the EU directives (*i.e.*, hourly SO₂: 350 µg/m³; hourly NO₂: 200 µg/m³; mean 8hourly O₃: 180 µg/m³; daily PM₁₀: 50 µg/m³).

Katsoulis and Kassomenos (2004) gave the following description of stress categories scale for daily AQSI: (i) Class I (AQSI < 0.2): “Very Low” (ii) Class II (0.2 < AQSI < 0.4): “Low”; (iii) Class III (0.4 < AQSI < 0.6): “Moderate”; (iv) Class IV (0.6 < AQSI < 0.8): “Distinct”; (v) Class V (0.8 < AQSI < 1): “Strong” and, finally, (vi) Class VI (AQSI > 1): “Extreme”.

Pearson correlation coefficients were used to investigate the pair-wise relationship between air temperature, relative air humidity, air pollutant concentrations, the contribution of each pollutant in the AQSI and daily AQSI values. The confidence level was set at $p = 0.05$. Since the scope of this paper is to examine the contribution of PM₁₀ to the daily AQSI and to identify non-local dust sources, when the upper thresholds of AQSI were exceeded, then the ‘Flextra’ (Air mass trajectories) model was used to calculate air masses back trajectories, their origin and the type of weather systems occurred. FLEXTRA is an atmospheric trajectory model. It can compute both forward and backward trajectories and can be driven by meteorological input data from a variety of global and regional models including ECMWF analyses and forecasts (Stohl, 1998).

3. Results and discussion

All the available air pollutants data per day were used for the calculation of the daily AQSI and descriptive statistics were provided separately for each pollutant and the composite index (Tab. 1). Sulphur dioxide (SO₂) concentrations, both average and maximum daily or hourly values, have been greatly reduced since the 1980s over the entire study, and are now well below the EU Directive threshold. There are very few and short terms exceeding of thresholds, so a limited contribution of this air pollutant to daily AQSI values was observed.

Nitrogen dioxide (NO₂) concentrations remained quite stable throughout the study period, being systematically under the threshold defined by CEC Directive 99/30 – both as average values and extremes. Although the meteorological conditions in the area – especially during morning hours (morning calms, weak sea breeze) – led to high NO₂ concentrations, only rare exceeding of the normative threshold was recorded.

The study area is also featuring (HNMS, 2021) high insolation (about 2,800 hours of sunshine per year) and considerable air temperature (mean value for summer months: 27.8 °C), stimulating formation and consolidation of photochemical pollution. Ozone (O₃), due to its photochemical nature, shows a marked seasonal trend, depending on solar irradiation. During summer months, the 8-hours moving average exceeded the EU threshold. Ozone, as linked to specific sources (Lykoudis et al., 2008).

Table 1. Descriptive statistics of daily values of the air pollutants, the Air Quality Stress Index (AQSI), and number of exceedings, distinguishing two thresholds (0.8 and 1) in Aspropyrgos, by year.

		2012	2013	2014	2015	2016	2017	2018	2019	2020
SO ₂	Average	8	6	6	8	7	7	6	6	10
	StDev	10	5	6	8	8	5	5	4	6
	Min	0	0	1	1	1	0	0	1	2
	Max	62	28	55	57	57	30	28	21	52
NO ₂	Average	35	48	36	41	51	39	46	47	41
	StDev	16	22	14	17	18	14	15	16	15
	Min	3	8	5	5	16	8	13	14	10
	Max	81	140	92	90	110	77	94	101	92
O ₃	Average	36	41	50	54	42	43	44	33	46
	StDev	20	24	23	23	23	20	21	20	22
	Min	3	1	4	11	8	5	2	2	2
	Max	91	102	100	114	240	94	93	84	91
PM ₁₀	Average	58	54	52	41	47	42	49	49	42
	StDev	20	21	51	16	23	17	25	20	18
	Min	24	11	9	15	14	8	11	8	3
	Max	113	154	726	124	283	112	310	123	115
AQSI	Average	0.32	0.44	0.42	0.42	0.45	0.41	0.44	0.48	0.41
	StDev	0.14	0.16	0.25	0.12	0.15	0.12	0.15	0.17	0.13
	Min	0.10	0.06	0.02	0.14	0.16	0.18	0.14	0.09	0.12
	Max	0.81	1.19	3.90	0.84	1.70	0.89	1.78	1.25	0.94
AQSI ≥ 0.8		1	8	6	1	5	1	5	16	4
AQSI ≥ 1		0	2	3	0	2	0	2	2	0

PM₁₀ concentrations in Aspropyrgos represent the most important pollutant in the area, maintaining very high for both daily and hourly values (Tab. 1) and the respective thresholds were frequently exceeded. According to earlier studies (Abatzoglou et al., 1996; Razos and Christides, 2010), PM₁₀ corresponds to 80% of the Total Suspended Particulate (TSP) in the area. The relative and cumulative frequency [%] of PM₁₀ classes [$\mu\text{g}/\text{m}^3$] during 2012–2020 in Aspropyrgos was shown in Fig. 2. Only 43% of the recorded PM₁₀ daily values were below the EU threshold ($50 \mu\text{g}/\text{m}^3$). All the remaining records exceeded largely this threshold. Although earlier studies (Flocas et al., 2009; Dimitriou and Kassomenos, 2017; Matthaïos et al., 2017) have reported similar cases from other sites in the Eastern Mediterranean basin, a persistence over time of particularly high values was observed in the study area.

Pearson correlation coefficients (Tab. 2) were calculated for the association between air temperature (T_a), relative humidity (RH), air pollutant concentrations (SO₂, NO₂, O₃, PM₁₀), considering both average and maximum values, the contribution of each pollutant to daily AQSI (AQ_{xx}), as well as and the AQSI

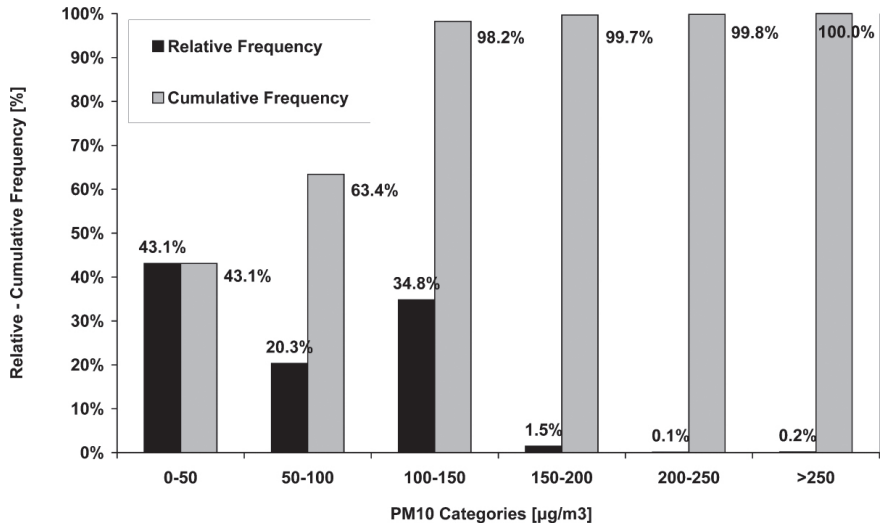


Figure 2. Relative and cumulative frequency [%] of PM10 categories [µg/m³] of recorded values, during the 2012–2020 measurement campaign in the municipality of Aspropyrgos.

itself. Positive and statistically significant coefficients were shown in bold and negative, statistically significant, coefficients were marked with italics and light grey. An intense correlation between ozone and air temperature was demonstrated, together with the strong dependence of the AQSI from PM₁₀. The esti-

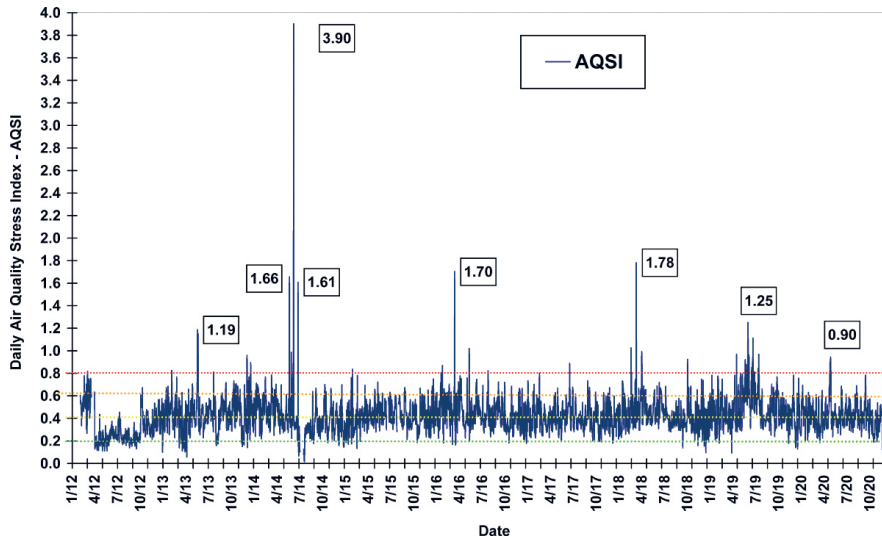


Figure 3. Variation of daily Air Quality Stress Index (AQSI) values. Thresholds of the index are marked with green, yellow, orange, and red lines.

Table 2. Pearson correlation coefficients investigating the association between air temperature (Ta), relative air humidity (RH), air pollutant concentrations (SO₂, NO₂, O₃, PM₁₀)—both average and maximum values, the contribution of each pollutant to daily Air Quality Stress Index (AQSI) and the AQSI. Positive and statistically significant coefficients are shown in bold; negative, statistically significant coefficients are shaded with italics and light grey (Abbreviations: Ta, air temperature; RH, relative humidity; SO₂, sulphur dioxide; NO₂, nitrogen dioxide; O₃, ozone; PM₁₀, particulate matter less than 10 µm in diameter; AQ_SO₂, contribution of SO₂; AQ_NO₂, contribution of NO₂; AQ_O₃, contribution of O₃; AQ_PM₁₀, contribution of PM₁₀).

	Tav	Tmax	RHav	RHmax	SO ₂ av	SO ₂ max	NO ₂ av	NO ₂ max	O ₃ av	O ₃ max	PM ₁₀ av	PM ₁₀ max	AQ_SO ₂	AQ_NO ₂	AQ_O ₃	AQ_PM ₁₀
Tmax	0.99															
RHav	<i>-0.62</i>	<i>-0.64</i>														
RHmax	<i>-0.60</i>	<i>-0.60</i>	0.92													
SO ₂ av	-0.01	0.04	0.02	0.02												
SO ₂ max	-0.04	0.01	0.02	0.03	0.82											
NO ₂ av	-0.06	-0.01	0.18	0.18	0.31	0.27										
NO ₂ max	0.01	0.07	0.07	0.10	0.30	0.26	0.86									
O ₃ av	0.61	0.59	<i>-0.67</i>	<i>-0.63</i>	<i>-0.15</i>	<i>-0.11</i>	<i>-0.51</i>	-0.31								
O ₃ max	0.59	0.61	<i>-0.54</i>	<i>-0.49</i>	0.05	0.07	-0.19	0.00	0.82							
PM ₁₀ av	-0.03	0.00	0.19	0.19	0.22	0.20	0.39	0.33	-0.33	-0.12						
PM ₁₀ max	-0.02	0.01	0.19	0.22	0.17	0.14	0.31	0.30	-0.27	-0.08	0.79					
AQSI_SO ₂	-0.02	-0.02	0.00	0.00	0.23	0.44	0.02	0.01	-0.01	-0.01	0.00	-0.01				
AQSI_NO ₂	-0.02	0.02	0.06	0.07	0.25	0.22	0.64	0.75	-0.21	0.00	0.26	0.24	0.03			
AQSI_O ₃	0.40	0.41	-0.37	-0.35	0.06	0.06	-0.10	0.01	0.48	0.54	-0.03	-0.05	-0.01	-0.01		
AQSI_PM ₁₀	0.04	0.06	0.07	0.08	0.18	0.14	0.30	0.25	-0.23	-0.07	0.85	0.66	-0.01	0.18	-0.01	
AQSI	0.14	0.18	0.03	0.05	0.36	0.36	0.51	0.54	-0.17	0.11	0.92	0.73	0.06	0.42	0.17	0.79

mated correlation coefficients with AQSI was 0.72, 0.79, and 0.92, respectively for AQ_PM₁₀, PM₁₀max, and PM₁₀av.

The diurnal variation of the daily AQSI was illustrated together with air quality thresholds (classes, see above) using colored lines (Fig. 3). Most of the recorded values was classified as “Moderate” and “Strong”. Since a basic assumption of our study is that PM₁₀ concentrations play a role in the annual variation

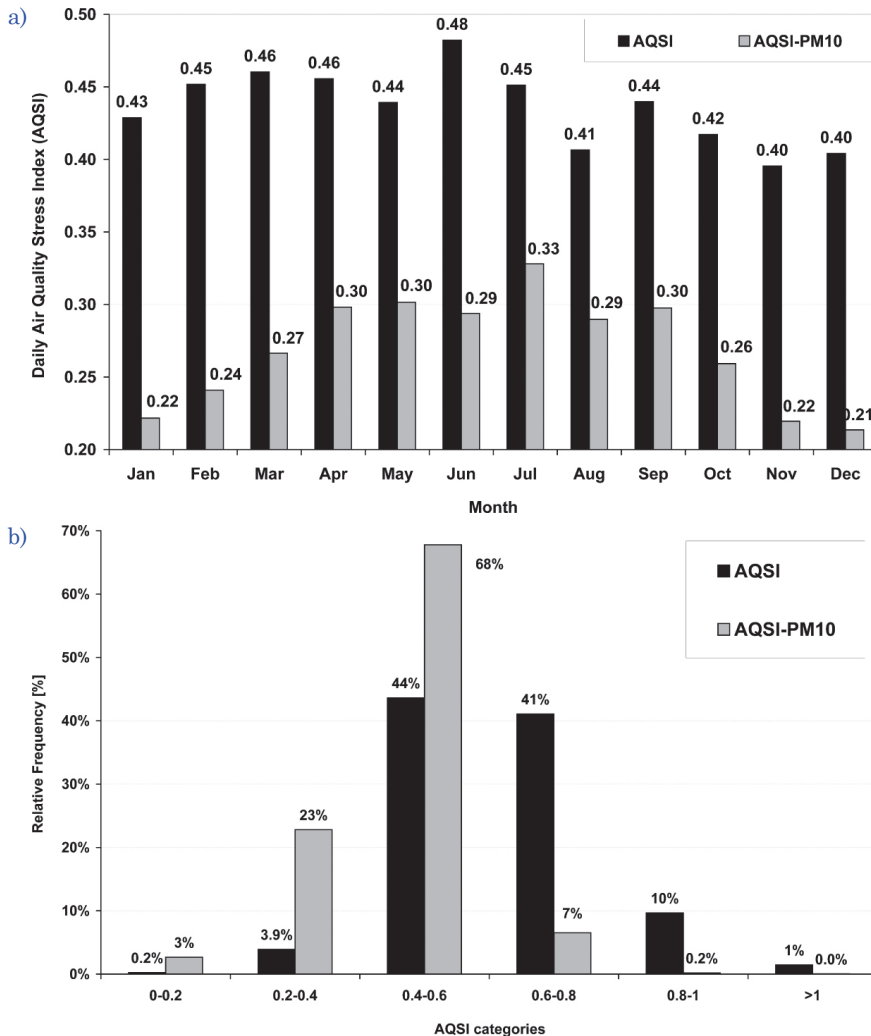


Figure 4. a) Month means of the daily Air Quality Stress Index with (black bars) and without (light gray bars) the contribution of PM₁₀ air pollutant to index values. b) Relative Frequency of values with (black bars) and without (light gray bars) the contribution of PM₁₀ air pollutant to AQSI classes, during the 2012–2020 measurement campaign in the municipality of Aspropyrgos.

of the index, the AQSI was recalculated excluding the PM₁₀ (AQSI-PM₁₀) values. According to the results shown in Fig. 4, the AQSI-PM₁₀ had a clear annual variation, with a peak during summer months and a low during winter months. On the contrary, AQSI showed a weak annual variation, with slightly higher values during spring months. The contribution of PM₁₀ to the daily AQSI range was estimated in a range between 17% and 90%. In agreement with other studies (Koukoulakis et al., 2019; Kanellopoulos et al. 2021), it was documented how PM₁₀ was documented to have a daily impact to local air quality.

As illustrated in Fig. 3, the 0.8 EU threshold was overpassed frequently, delineating a strong health risk. A total of 47 exceeding events was identified, and 17 events exceeded a higher threshold (1), with a peak of 3.9.

Air masses back trajectories (Fig. 5) were generated using the Flextra model, which use meteorological data provided by ECMWF (European Centre for Medium Range Weather Forecast; www.nilu.no/trajectories; Stohl, 1998).

Results for 45 events from the 47 cases described above suggest that air masses transportation originated mainly from Sahara Desert and usually they circulated above central Mediterranean Sea and Greece, in agreement with previous studies (Aleksandropoulou and Lazaridis, 2013; Nastos, 2012). Two major types of circulation were identified (cyclonic and anti-cyclonic, and variations concerning the strengths of each observed system were frequently observed (Flocas et al., 2009; Nastos et al., 2011; Khomsi et al., 2020). Air masses above Mediterranean Sea usually transport significant amounts of Sahara dust and, at the same time, they enrich hot dry air with humidity (Kassomenos et al., 1998; Dimitriou and Kassomenos, 2017), having in turn a significant impact on human perception of weather conditions (Pantavou and Mavrakis, 2015; Pantavou et al., 2018; Cori et al., 2020). World Meteorological Organization (WMO, 2021) mentioned that dust transport episodes can be characterized as a hazard, for which official guidelines for preparation and mitigation of such events are largely unavailable (Palmos et al., 2021). Also, during the last few years, early-summer heat waves occurred in Greece, being accompanied with intense dust transport episodes. Those weather condition downgraded air quality (Trianti et al., 2017; Mavrakis et al., 2021) and alarmed authorities.

Air masses back trajectories were shown in correspondence with the three highest values of AQSI (a to c) and the main source areas were shown in Figs. 5d to 5f. The highest value of AQSI was recorded in 2014, June, the 12th, reaching 3.90 (Categorie 'Extreme – VI'). During all the day, the average and maximum recorded values were the same (726 µg/m³), and the episode was associated with anti-cyclonic conditions (a high pressure system dominated in Central Mediterranean Sea). This was one of the longer lasting dust transport episode recorded during measurement campaigns. During this episode lasting from May 25th to June 12th, 2014, two times maximum hourly values of the PM₁₀ were recorded equal to 921 µg/m³. The second extreme case (AQSI = 1.78) was recorded in 2018, March, the 26th (Fig. 5b), and it was associated with cyclonic conditions

(a deep low pressure system located west of Greece in Central Mediterranean Sea). PM_{10} average daily value was $310 \mu\text{g}/\text{m}^3$ and the maximum hourly value was $525 \mu\text{g}/\text{m}^3$. The third episode (AQSI = 1.70) was recorded in 2016, March, the 23th (Fig. 5c) and it was associated with cyclonic conditions (a shallow low

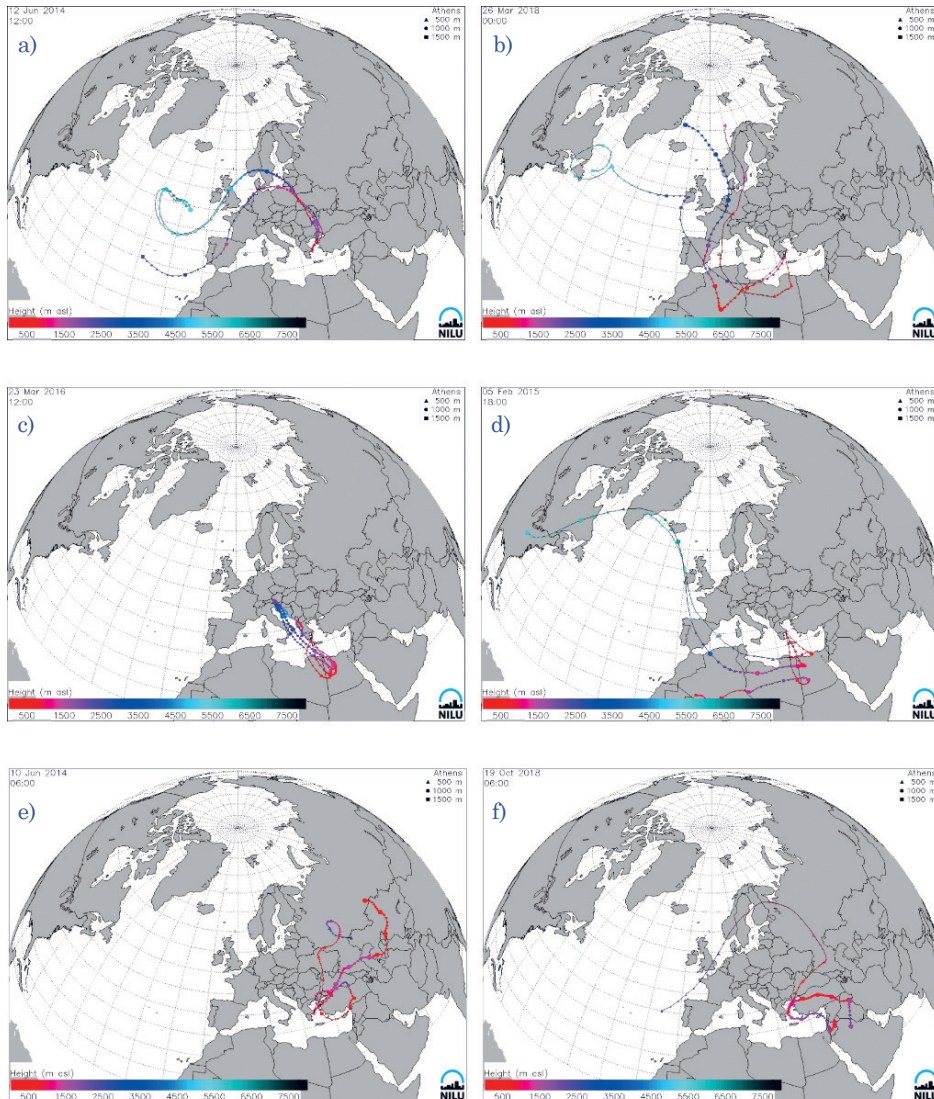


Figure 5. Air masses back trajectories for (i) the highest values of AQSI: a) 12/06/2014 at 12:00 UTC; b) 23/03/2016 at 12:00 UTC; c) 26/03/2018 at 00:00 UTC, and for (ii) transport area sources: d) (Sahara desert) 05/02/2021 at 18:00 UTC; e) (Central Asia desert) 10/06/2014 at 06:00 UTC; f) (Middle East desert) 19/10/2018 at 06:00 UTC.

pressure system moving across North Africa seashore). PM₁₀ average daily value was 283 µg/m³, while the maximum hourly value approached 904 µg/m³.

As far as transport area sources, North Africa region/Sahara desert was the mean source of dust transport in 45 out of 47 cases (a typical example was the case of 2021, February, the 5th, Fig. 5d). Air mass back trajectories identified one case of dust transport from Central Asia deserts in 2014, June, the 10th (Fig. 5e) and one case of dust transport from Middle East deserts in 2018, October, the 19th (Fig. 5f).

4. Discussion

Our study has investigated the contribution of PM₁₀ air pollutant to daily Air Quality Stress Index in the socio-environmentally stressed industrial city of Aspropyrgos located in Western Attica, Greece, regarded as the most powerful pollution source of Athens. The results indicate that more than 55% of PM₁₀ values exceeded the EU threshold. This made PM₁₀ concentrations the main contributor to AQSI levels. Excluding PM₁₀, the daily values of AQSI remained always below the normative threshold and showed a clear annual variability. Including PM₁₀ values, the AQSI showed a weak annual variability with a spring peak. To identify the source of PM₁₀ values under exceeding of the AQSI upper threshold, the Flextra model was used. Results show that dust transport episodes mainly from Sahara desert, is a natural contributor to the daily levels of PM₁₀ and AQSI levels and those episodes reach their peak during spring and autumn months.

The results from the present study are in agreement with previous studies (Cori et al., 2020) and could be used in environmental awareness campaigns informing population about the negative consequences of PM₁₀ / dust transport episodes and alerting citizens toward adoption of individual prevention measures. The empirical results of this study indicate that policy makers have to consider additional prevention and mitigation plans to meet new health risks for general population regarding PM₁₀ concentrations. This could also be a planning and risk management tool for policy and decision making authorities to chart their long-term future actions with a better understanding of potentially unfolding scenarios and their impacts.

Acknowledgement – NILU is acknowledged for providing the FLEXTTRA trajectories (www.nilu.no/trajectories) used in this study.

References

- Abatzoglou, G., Chaloulakou, A., Assimacopoulos, D. and Lekkas, T. (1996): Prediction of air pollution episodes: Extreme value theory applied in Athens, *Environ. Technol.*, **17**, 349–359, <https://doi.org/10.1080/09593331708616394>.

- Aleksandropoulou, V. and Lazaridis, M. (2013): Identification of the influence of African dust on PM10 concentrations at the Athens air quality monitoring network during the period 2001–2010, *Aerosol Air Qual. Res.*, **13**, 1492–1503, <https://doi.org/10.4209/aaqr.2012.12.0363>.
- CEC (2001): Commission Directive of 17 October 2001 amending Annex V to Council Directive (1999/30/EC) relating to limit values for sulphur dioxide, nitrogen dioxide and oxides of nitrogen, particulate matter and lead in ambient air. *Official Journal of the EC*, L 278/35.
- Cecchini, M., Zambon, I., Pontrandolfi, A., Turco, R., Colantoni, A., Mavrakakis, A. and Salvati, L. (2019): Urban sprawl and the ‘olive’ landscape: Sustainable land management for ‘crisis’ cities, *GeoJournal*, **84**, 237–255, <https://doi.org/10.1007/s10708-018-9848-5>.
- Cori, L., Donzelli, G., Gorini, F., Bianchi, F. and Curzio, O. (2020): Risk perception of air pollution: A systematic review focused on particulate matter exposure, *Int. J. Env. Res. Pub. He.*, **17**(17), 6424, <https://doi.org/10.3390/ijerph17176424>.
- Di Felicianantonio, C., Salvati, L., Sarantakou, E. and Rontos, K. (2018): Class diversification, economic growth and urban sprawl: Evidences from a pre-crisis European city, *Qual. Quant.*, **52**, 1501–1522, <https://doi.org/10.1007/s11135-017-0532-5>.
- Dimitriou, K. and Kassomenos, P. (2017): Aerosol contributions at an urban background site in Eastern Mediterranean – Potential source regions of PAHs in PM₁₀ mass, *Sci. Total Environ.*, **598**, 563–571, <https://doi.org/10.1016/j.scitotenv.2017.04.164>.
- Flocas, H., Kelessis, A., Helmis, C., Petrakakis, M., Zoumakis, M. and Pappas, K. (2009): Synoptic and local scale atmospheric circulation associated with air pollution episodes in an urban Mediterranean area, *Theor. Appl. Climatol.*, **95**, 265–277, <https://doi.org/10.1007/s00704-008-0005-9>.
- Hellenic National Meteorological Service (HNMS) (2021): Climate of Greece, http://www.hnms.gr/emv/el/climatology/climatology_city?perifereia=Attiki&poli=Elefsina (last accessed on June 1, 2021).
- Hellenic Statistical Authority (ELSTAT) (2021): Demographic characteristics, <https://www.statistics.gr/> (last accessed on 1 June 2021)
- Kanellopoulos, P. G., Verouti, E., Chrysochou, E., Koukoulakis, K. and Bakeas, E. (2021): Primary and secondary organic aerosol in an urban/industrial site: Sources, health implications and the role of plastic enriched waste burning, *J. Environ. Sci.*, **99**, 222–238, <https://doi.org/10.1016/j.jes.2020.06.012>.
- Karavas, Z., Karayannis, V. and Moustakas, K. (2021): Comparative study of air quality indices in the European Union towards adopting a common air quality index, *Energ. Environ.-UK*, **32**, 959–980, <https://doi.org/10.1177/0958305X20921846>.
- Kassomenos, P. A., Flocas, H. A., Lykoudis, S. and Skouloudis, A. (1998): Spatial and temporal characteristics of the relationship between air quality status and mesoscale circulation over an urban Mediterranean basin, *Sci. Total Environ.*, **217**, 37–57, [https://doi.org/10.1016/S0048-9697\(98\)00167-3](https://doi.org/10.1016/S0048-9697(98)00167-3).
- Kassomenos, P. A., Kelessis, A., Petrakakis, M., Zoumakis, N., Christidis, Th., A. K. and Paschalidou, A. K. (2012): Air quality assessment in a heavily polluted urban Mediterranean environment through air quality indices, *Ecol. Indic.*, **18**, 259–268, <https://doi.org/10.1016/j.ecolind.2011.11.021>.
- Katsoulis, B. D. and Kassomenos, P. A. (2004): Assessment of the air-quality over urban areas by means of biometeorological indices: The case of Athens, Greece, *Environ. Technol.*, **25**, 1293–1304, <https://doi.org/10.1080/09593332508618375>.
- Khomsy, K., Najmi, H., Chelhaoui, Y. and Souhaili, Z. (2020): The contribution of large-scale atmospheric patterns to pollution with PM10: The new Saharan Oscillation Index, *Aerosol Air Qual. Res.*, **20**, 1038–1047, <https://doi.org/10.4209/aaqr.2019.08.0401>.
- Koukoulakis, K. G., Chrysohou, E., Kanellopoulos, P. G., Karavoltos, S., Katsouras, G., Dassenakis, M., Nikolelis, D. and Bakeas, E. (2019): Trace elements bound to airborne PM10 in a heavily industrialized site nearby Athens: Seasonal patterns, emission sources, health implications, *Atmos. Pollut. Res.*, **10**, 1347–1356, <https://doi.org/10.1016/j.apr.2019.03.007>.

- Lykoudis, S., Psounis, N., Mavrakis, A. and Christides, A. (2008): Predicting photochemical pollution in an industrial area, *Environ. Monit. Assess.*, **142**, 279–288, <https://doi.org/10.1007/s10661-007-9925-6>.
- Matthaios, V. N., Triantafyllou, A. G. and Koutrakis, P. (2017): PM10 episodes in Greece: Local sources versus long-range transport — Observations and model simulations, *J. Air Waste Manage.*, **67**, 105–126, <https://doi.org/10.1080/10962247.2016.1231146>.
- Mavrakis, A., Kapsali, A., Tsiros, I. X. and Pantavou, K. (2021): Air quality and meteorological patterns of an early spring heatwave event in an industrialized area of Attica, Greece, *Euro-Mediterr. J. Environ. Integr.*, **6**, 25, <https://doi.org/10.1007/s41207-020-00237-0>.
- Mavrakis, A., Lykoudis, S., Christides, A., Dasaklis, S., Tasopoulos, A., Theoharatos, G., Kyvelou, S. and Verouti, E. (2008): Air quality levels in a closed industrialized basin (Thriassion Plain, Greece), *Fresen. Environ. Bull.*, **17**, 443–454.
- Mavrakis, A., Papavasileiou, C. and Salvati, L. (2015a): Towards (un)sustainable urban growth? Climate aridity, land-use changes and local communities in the industrial area of Thrasio plain, *J. Arid Environ.*, **121**, 1–6, <https://doi.org/10.1016/j.jaridenv.2015.05.003>.
- Mavrakis, A., Salvati, L. and Flocas, H. (2015b): Mixing ratio as indicator of climate variations at a local scale: trends in an industrial area of the Eastern Mediterranean, *Int. J. Climatol.*, **36**, 1534–1538, <https://doi.org/10.1002/joc.4410>.
- Mavrakis, A., Rontos, K., Chronopoulou, C. and Salvati, L. (2016): Population dynamics, industrial development and the decline of the traditional agro-forest landscape on the Mediterranean urban fringe: A case study in Greece, *Int. J. Sust. Dev.*, **19**, 1–14, <https://doi.org/10.1504/IJSD.2016.073649>.
- Mavrakis, A., Salvati, L., Kyvelou, S., Tasopoulos, A., Christides, A., Verouti, E., Liakou, M., Cividino, S., Zambon, I. and Papavasileiou, C. (2020): Social contexts, local practices, and urban projects for a bioregional postcrisis recovery: The emblematic example of Athens' fringe, Greece, in: *Bioregional planning and design: Volume II*, edited by Fanfani, D. and Matarán Ruiz, A. Springer, Cham, https://doi.org/10.1007/978-3-030-46083-9_7.
- Mayer, H., Makra, L., Kalberlah, F., Ahrens, D. and Reuter, U. (2004): Air stress and air quality indices, *Meteorol. Z.*, **13**, 395–403, <https://doi.org/10.1127/0941-2948/2004/0013-0395>.
- Nastos, P. T. (2012): Meteorological patterns associated with intense Saharan dust outbreaks over Greece in winter, *Adv. Meteorol.*, 828301, <https://doi.org/10.1155/2012/828301>.
- Nastos, P. T., Kampanis, N. A., Giaouzaki, K. N. and Matzarakis, A. (2011): Environmental impacts on human health during a Saharan dust episode at Crete Island, Greece, *Meteorol. Z.*, **20**, 517–529, <https://doi.org/10.1127/0941-2948/2011/0246>.
- Palmos, D., Papavasileiou, C., Papakitsos, C. E., Vamvakeros, X. and Mavrakis, A. (2021): Enhancing the environmental programmes of secondary education by using web-tools concerning precaution measures in civil protection: The case of Western Attica (Greece), *Safety Sci.*, **135**, 105117, <https://doi.org/10.1016/j.ssci.2020.105117>.
- Pantavou, K. and Mavrakis, A. (2015): Thermal perception of teenagers in a cool outdoor environment – A case study, *Geofizika*, **32**, 79–92, <https://doi.org/10.15233/gfz.2015.32.1>.
- Pantavou, K., Psiloglou, B., Lykoudis, S., Mavrakis, A. and Nikolopoulos, G. K. (2018): Perceived air quality and particulate matter pollution based on field survey data during a winter period, *Int. J. Biometeorol.*, **62**, 2139–2150, <https://doi.org/10.1007/s00484-018-1614-3>.
- Razos, P. and Christides, A. (2010): An investigation on heavy metals in an industrial area in Greece, *Int. J. Environ. Res.*, **4**(4), 785–794, <https://doi.org/10.22059/ijer.2010.265>.
- Salvati, L. and Mavrakis, A. (2014): Narrative and quantitative analysis of human pressure, land-use and climate aridity in a transforming industrial basin in Greece, *Int. J. Environ. Res.*, **8**, 115–122, <https://doi.org/10.22059/ijer.2014.700>.
- Stohl, A. (1998): Computation, accuracy and applications of trajectories – A review and bibliography, *Atmos. Environ.*, **32**, 947–966, [https://doi.org/10.1016/S1352-2310\(97\)00457-3](https://doi.org/10.1016/S1352-2310(97)00457-3).
- Toumpos, M., Flocas, H. A., Christides, A. and Mavrakis, A. (2017): Generating a “Typical Air Pollutant Day” in Thrasio Plain, Greece, in: *Perspectives on Atmospheric Sciences*, edited by Kara-

- costas, T., Bais, A. and Nastos, P. Springer Atmospheric Sciences. Springer, Cham, https://doi.org/10.1007/978-3-319-35095-0_154.
- Trianti, S. M., Samoli, E., Rodopoulou, S., Katsouyanni, K., Papiris, S. A. and Karakatsani, A. (2017): Desert dust outbreaks and respiratory morbidity in Athens, Greece, *Environ. Health*, **16**, 72, <https://doi.org/10.1186/s12940-017-0281-x>.
- Urban Atlas of European Environmental Agency (2016): <http://www.eea.europa.eu/data-and-maps/data/urban-atlas> (last accessed on June 1, 2021).
- World Meteorological Organization (WMO) (2021): Sand and dust storm warning advisory and assessment system. *WMO Airborne Dust Bulletin*, **5**, July 2021, WMO Airborne Dust Bulletin | E-Library (last accessed on July 8, 2021).

SAŽETAK

PM₁₀ i indeks pritiska onečišćenjem zraka u industrijskom gradu na istočnom Sredozemlju*Eleni Verouti, Dimitrios Gavathas i Anastasios Mavrakis*

Ispitan je doprinos PM₁₀ dnevnom indeksu pritiska onečišćenjem zraka (AQSI) u industrijskom gradu na istočnom Sredozemlju (Aspropyrgos, Grčka). S tim ciljem analizirane su satne vrijednosti koncentracija četiriju polutanata (SO₂, NO₂, O₃ i PM₁₀) za razdoblje od 2012. do 2020. Rezultati su pokazali da razinama AQSI najviše doprinose PM₁₀ (između 17% i 90% za dnevne vrijednosti AQSI) uz umjerenu godišnju varijabilnost i proljetni maksimum. Ako se iz analize izuzmu PM₁₀, vrijednosti AQSI uvijek ostaju ispod praga od 0.8. Kako bi se identificirali izvori epizoda PM₁₀, na 47 slučajeva u kojima je prekoračen gornji prag, primijenjen je model putanja česti zraka – Flextra. Rezultati modela pokazuju da epizode transporta prašine, prvenstveno iz Sahare, doprinose dnevnom razinama PM₁₀ i, u skladu s tim, razinama AQSI.

Ključne riječi: PM₁₀, indeks pritiska onečišćenjem zraka, epizode transporta prašine

Corresponding author's address: Anastasios Mavrakis, Environmental Education Coordinator, West Attica Secondary Education Directorate, Greek Ministry of Education, 24 I. Dragoumi str., GR–19200, Elefsis – Attica, Greece; e-mail: mavrakisan@yahoo.gr



This work is licensed under a Creative Commons Attribution-NonCommercial 4.0 International License.